Comments on "Variations of Joint Integrated Data Association with Radar and Target-Provided Measurements"

Domenico Gaglione, Paolo Braca, Giovanni Soldi, Florian Meyer, Audun G. Hem, Edmund F. Brekke, and Franz Hlawatsch

***Abstract*—Recently, a method for including target-provided measurements within a joint integrated probabilistic data association (JIPDA) filter was presented and compared with a belief propagation (BP) based multi-target tracking method. While the JIPDA-based approach uses multiple kinematic models within an interacting multiple models (IMM) framework, the BP-based approach uses only a single kinematic model. Here, we present and analyze the results of similar experiments conducted on both simulated and real data. Our results show that the JIPDA-based method tends to outperform the BP-based method when the targets are well-separated and perform sharp maneuvers, whereas the BP-based method outperforms the JIPDA-based method when the targets are closely spaced.**

***Index Terms*—Multi-target tracking, data fusion, automatic identification system, sum-product algorithm, belief propagation, JIPDA filter, IMM framework**

I. Introduction

A. Background

In a recent publication [1], three methods for including target-provided measurements in a joint integrated probabilistic data association (JIPDA) framework were proposed. The framework considered in [1], referred to as VIMMJIPDA filter, combines interacting multiple models (IMM) and a visibility state within the well-established JIPDA filter [2]. The IMM concept, first introduced in [3], allows the use of multiple kinematic models for the tracking of maneuvering targets, while the visibility state indicates whether the tracked target is visible to the sensor or not. A target-provided measurement is an observation produced by a target and made available to the tracking method. This observation usually includes kinematic information, e.g., the target's position and velocity, and additional information such as a unique code identifying the target. The target obtains its own position and velocity through an onboard device, generally a global navigation satellite system transponder, and transmits this information as well as any other relevant information to neighboring targets and to a central fusion node. Examples of such systems are the automatic identification system (AIS) for maritime surveillance and vessel collision avoidance [4] and the automatic dependent surveillance broadcast (ADS-B) system for air traffic control [5].

These target-dependent reporting systems differ from classical perception sensors such as radar, lidar, and camera in several aspects. Firstly, the measurements they produce are asynchronous, because they are provided by the targets themselves and each target can transmit its messages at any time. Secondly, a target-provided measurement cannot be a false alarm, because it is not the result of a detection process.[1] Several attempts have been made to fuse target-provided measurements and observations produced by perception sensors. One common approach is to consider the reporting system and the perception sensor as stand-alone assets, and accordingly estimate two separate sets of tracks which are later fused to form a single set of estimated tracks. This approach, which is known as track-level fusion, has some performance limits compared to measurement-level fusion techniques [6].

The methods proposed in [1] follow a measurement-level fusion approach and are based on the VIMMJIPDA tracking method. Specifically, three different methods for handling the target-provided measurements are proposed. One of them processes the measurements as they arrive, i.e., sequentially; the others collect the measurements and process them at fixed times. The validity of these approaches is demonstrated both in a simulated maritime scenario and with real data acquired as part of the Autosea project conducted by the Norwegian University of Science and Technology [7], and the performance of the proposed methods is compared with that of the belief propagation (BP) based tracking method with target-provided measurement fusion capabilities presented in [8], [9]. The setup of both the simulated scenario and the real experiment consists of a single radar sensor and the AIS. It is observed that the particle filter (PF) implementation of the BP-based tracking method (referred to as the BP-PF+AIS method) performs worse than the VIMMJIPDA-based methods and, in some cases, even worse than a radar-only method, i.e., a method that uses only the radar measurements.

This work was supported in part by the NATO Allied Command Transformation (ACT) under the DKOE project, in part by the Austrian Science Fund (FWF) under grant P 32055–N31, in part by the Research Council of Norway through Project 295033 Autosit, in part by DNV, in part by Kongsberg, and in part by Maritime Robotics.

D. Gaglione, P. Braca, and G. Soldi are with the NATO Centre for Maritime Research and Experimentation (CMRE), La Spezia, Italy (e-mail: domenico.gaglione@cmre.nato.int, paolo.braca@cmre.nato.int, giovanni.soldi@cmre.nato.int).

F. Meyer is with the Scripps Institution of Oceanography and the Department of Electrical and Computer Engineering, University of California San Diego, La Jolla, CA, USA (e-mail: flmeyer@ucsd.edu).

A. G. Hem and E. F. Brekke are with the Department of Engineering Cybernetics, Norwegian University of Science and Technology, Trondheim, Norway (e-mail: audun.g.hem@ntnu.no, edmund.brekke@ntnu.no).

F. Hlawatsch is with the Institute of Telecommunications, TU Wien, Vienna, Austria (e-mail: franz.hlawatsch@tuwien.ac.at).

[1] Nevertheless, target-dependent reporting systems like the AIS can be subject to intentional reporting of false information. However, this is not taken into account in [1] nor in the remainder of this paper.

B. Contribution

The implementation of the BP-PF+AIS method is not publicly available, which led the authors of [1] to use their own implementation. In this paper, we study the performance of the original implementation of the BP-PF+AIS method used in [8], [9] for a simulated scenario similar to the one described in [1, Sec. VIII-A], as well as on the real dataset provided by the Autosea project [7]. Additionally, we consider the simulated scenario described in [9, Sec. VI-A]. The performance obtained with the original implementation of the BP-PF+AIS method is compared with that obtained with the original VIMMJIPDA method using only the radar measurements [2] and with the sequential method proposed in [1] (to be referred to as VIMMJIPDA+AIS), for which code is available in [10]. We note that the BP-PF+AIS method described in [8], [9] does not use multiple kinematic models. However, a BP-based tracking method using multiple kinematic models that conforms to the general IMM approach is presented in [11]. Therefore, we also evaluate and compare the performance of the BP-PF+AIS method described in [8], [9] properly extended to exploit multiple kinematic models as proposed in [11]; we briefly refer to this version as BP-PF+AIS+IMM method. We will demonstrate that while the BP-PF+AIS and BP-PF+AIS+IMM methods have performance advantages in the case of closely spaced targets, the VIMMJIPDA+AIS method performs better when the targets are well-separated and when they perform sharp maneuvers.

The remainder of this paper is organized as follows. Section II provides a brief description of the VIMMJIPDA, VIMMJIPDA+AIS, BP-PF+AIS, and BP-PF+AIS+IMM methods. Section III presents the results of an experimental comparison of these methods conducted on two simulated scenarios, while in Section IV the performance is compared on a real dataset. Concluding remarks are provided in Section V.

II. Brief Description of the Compared Methods

The VIMMJIPDA method, derived in [2] as a special case of the Poisson multi-Bernoulli filter, is a variation of the JIPDA filter for multi-target tracking that includes multiple kinematic models and a visibility state, and uses hypothesis enumeration to model the target-measurement data association. Specifically, a single-linkage clustering strategy is used to group targets that share measurements. Then, for groups with less than four targets or less than two measurements, brute-force hypothesis enumeration is performed, whereas Murty's algorithm [12] with a maximum of eight hypotheses is used for all other groups. The VIMMJIPDA+AIS method proposed in [1] builds upon [2] and incorporates target-provided measurements. One important technical detail that enables this is to model target birth as a marked Poisson point process, where the marks are constituted by the unique codes identifying the targets.

The BP-based multi-target tracking methods are described in [13] and references therein. The principle behind these methods is to exploit the statistical independence of certain random variables describing the tracking problem, and to represent these independence relationships by means of a factor graph. Then, using a message passing algorithm — i.e., the sum-product algorithm — on this factor graph enables an intuitive and computationally efficient approximation of the Bayesian inference needed for target detection and estimation. Fundamental for the derivation of these methods is to properly model and formulate the target-measurement data association. An iterative BP-based algorithm for data association with remarkable performance in terms of convergence and accuracy was proposed in [14]. A common approach to implementing BP-based tracking algorithms for general nonlinear/non-Gaussian kinematic and measurement models is to resort to a PF as described in [15].

Building upon [13]–[15], a suite of BP-PF methods have been recently developed. The BP-PF+AIS method proposed in [9] extends the previous works to incorporate heterogeneous data. This method fuses sensor measurements and target-provided measurements, e.g., AIS data, by establishing an appropriate likelihood for target-provided measurements and a statistical model for data association. A self-tuning BP-PF method that continuously adapts to time-varying system models is proposed in [11]. This method infers and adapts to an unknown detection probability of the sensors and employs multiple kinematic models in line with the IMM framework. Similar to a construction kit system, BP-based algorithm parts can be combined in a modular manner to achieve desired functionalities and properties. For example, the BP-PF+AIS+IMM method, which is used for comparison in this paper, combines the IMM framework proposed in [11] with the ability to fuse sensor measurements and target-provided measurements as established in [9].

III. Simulation Results

In this section, we present simulation results for the scenarios considered in [1, Sec. VIII-A] and [9, Sec. VI-A].

A. Scenario Considered in [1]

The simulated scenario considered in [1, Sec. VIII-A] employs a single radar sensor located at $[0, 0]^{\mathrm{T}}$ that surveys a circular area of radius 500 m with a time scan duration of 2.5 s. Five targets appear at the edge of that area, three at time $t = 0$ s and two at time $t = 10$ s, initially moving with a velocity of 3.75 m/s. The trajectories of the targets are generated according to a nearly constant velocity (NCV) kinematic model [16, Sec. 6.2.2] with driving noise variance set to 0.1^2 m^2 s^{-3}, and with occasional maneuvers according to a coordinated turn (CT) kinematic model [16, Sec. 4.2.2]. The radar detects a target with probability P_{D} and generates range-bearing measurements; the measurement noise is a two-dimensional (2D) zero-mean Gaussian random vector with covariance $\mathrm{diag}(8^2\,\mathrm{m}^2, 1^2\,\mathrm{deg}^2)$. The number of false alarms is Poisson distributed with mean 2. All targets provide AIS measurements containing their unique identifying code as well as their 2D Cartesian position and velocity. The number of AIS measurements provided by a target during each time scan is Poisson distributed with mean 0.5. The AIS measurement noise for position and velocity is a 4D zero-mean Gaussian random vector with covariance $\mathrm{diag}(3^2\,\mathrm{m}^2, 3^2\,\mathrm{m}^2, 0.1^2\,\mathrm{m}^2/\mathrm{s}^2, 0.1^2\,\mathrm{m}^2/\mathrm{s}^2)$. Fig. 1 shows a realization of the scenario with the

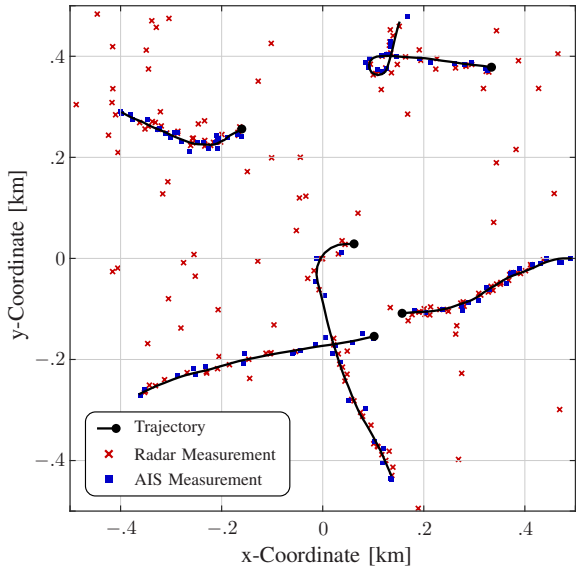

Fig. 1. A realization of the simulated scenario considered in [1, Sec. VIII-A], with $P_{\mathrm{D}} = 0.5$. The black dots indicate the final positions of the trajectories.

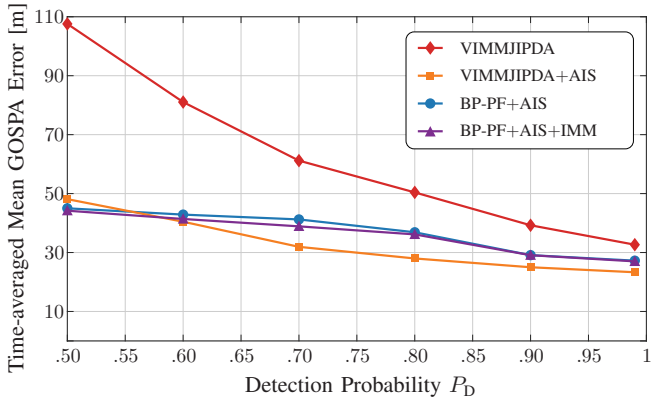

Fig. 2. Time-averaged mean GOSPA error versus detection probability P_{D} of the radar sensor for the simulated scenario considered in [1, Sec. VIII-A].

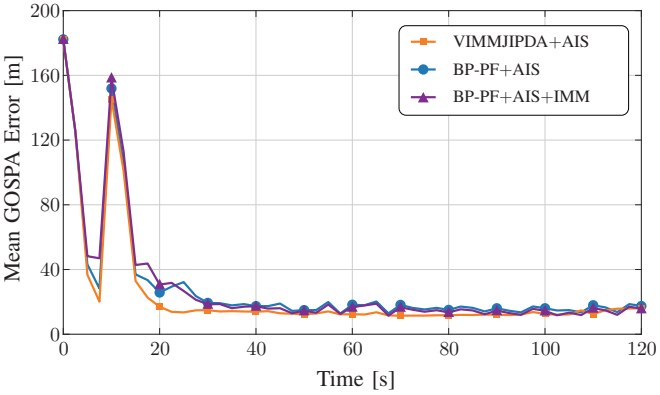

Fig. 3. Mean GOSPA error versus time for the simulated scenario considered in [1, Sec. VIII-A] with $P_{\mathrm{D}} = 0.9$.

trajectories of the five targets, the 2D position component of the AIS measurements, and the radar measurements generated with $P_{\mathrm{D}} = 0.5$.

In Figs. 2 and 3, we demonstrate and compare the performance of the radar-only method (i.e., VIMMJIPDA [2]), the sequential method proposed in [1] (i.e., VIMMJIPDA+AIS), the original implementation of the BP-PF+AIS method [8], [9], and the BP-PF+AIS+IMM method. The performance of these methods is measured by the mean generalized optimal sub-pattern assignment (GOSPA) error [17] of order 2 and with cut-off parameter 200 m, averaged over 100 simulation runs. The mean GOSPA error accounts for localization errors for correctly confirmed targets as well as for errors due to missed and false targets. For the VIMMJIPDA and VIMMJIPDA+AIS methods, we use the parameters reported in [1, Tab. III]. Where applicable, the same parameters are also used for the BP-PF+AIS and BP-PF+AIS+IMM methods (e.g., the survival probability), while parameters specifically related to the BP-based methods (e.g., the number of potential targets) are set as in [9]. The VIMMJIPDA and VIMMJIPDA+AIS methods use three models to characterize the kinematics of the targets, namely, two NCV models with different driving noise variances and one CT model. The BP-PF+AIS method uses a single NCV model; therefore, to account for potential maneuvers, the driving noise variance of the NCV model for the BP-PF+AIS method is set to 0.8^2 m^2 s^{-3}. Finally, the BP-PF+AIS+IMM method uses two NCV models with driving noise variance 0.05^2 m^2 s^{-3} and 0.8^2 m^2 s^{-3}. Differently from the NCV model, the CT model does not allow a simple closed-form calculation of the likelihood for the target-provided measurements specified in the supplementary material of [9]. Developing a tractable implementation of this likelihood is outside the scope of this paper, and for this reason the BP-PF+AIS+IMM method does not employ a CT model.

Fig. 2 shows the time-averaged mean GOSPA error when the detection probability P_{D} of the radar sensor is varied from 0.50 to 0.99. It can be seen that the VIMMJIPDA+AIS method performs better than both the BP-PF+AIS and BP-PF+AIS+IMM methods. Furthermore, the use of multiple NCV models within the BP-PF+AIS method offers only a marginal improvement. The difference in performance between the VIMMJIPDA+AIS method and the BP-PF+AIS and BP-PF+AIS+IMM methods can be explained by the fact that the VIMMJIPDA+AIS method uses also a CT model to better track maneuvering targets, and also by the fact that the BP-PF+AIS and BP-PF+AIS+IMM methods create a larger number of false tracks. However, differently from the results reported in [1], the time-averaged mean GOSPA error of the BP-PF+AIS method is lower than that of the VIMMJIPDA method.

Fig. 3 shows the mean GOSPA error versus time for $P_{\mathrm{D}} = 0.9$. Again differently from the results reported in [1], both the VIMMJIPDA+AIS method and the BP-PF+AIS and BP-PF+AIS+IMM methods correctly initialize the targets, as is demonstrated by their similar mean GOSPA errors at times $t = 0$ s and $t = 10$ s, i.e., when the targets appear. The slightly lower mean GOSPA error of the VIMMJIPDA+AIS method relative to the BP-PF+AIS and BP-PF+AIS+IMM methods can again be explained by the fact that the VIMMJIPDA+AIS method uses an additional CT model that al-

TABLE I
TIME-AVERAGED INDIVIDUAL COSTS CONSTITUTING THE MEAN GOSPA ERROR (IN METER) FOR THE SIMULATED SCENARIO CONSIDERED IN [1, SEC. VIII-A] WITH $P_{\mathrm{D}} = 0.9$. BOLD FONT HIGHLIGHTS THE LOWEST VALUE IN EACH COLUMN.

	LOCALIZATION	FALSE	MISSED
VIMMJIPDA+AIS	12.3	**0.3**	**12.7**
BP-PF+AIS	12.6	0.8	16.9
BP-PF+AIS+IMM	**11.2**	1.6	17.5

TABLE II
AVERAGE COMPUTATION TIMES (IN SECOND) PER TIME SCAN FOR THE SIMULATED SCENARIO CONSIDERED IN [1, SEC. VIII-A]. BOLD FONT HIGHLIGHTS THE LOWEST VALUE IN EACH COLUMN.

	P_{D}					
	.50	.60	.70	.80	.90	.99
VIMMJIPDA	.32	.31	.28	.28	.25	.26
VIMMJIPDA+AIS	.79	.70	.58	.57	.45	.46
BP-PF+AIS	**.20**	**.19**	**.20**	**.21**	**.21**	**.21**
BP-PF+AIS+IMM	.55	.53	.56	.56	.56	.56

lows it to maintain track continuity when targets maneuver, and by the larger number of false tracks created by the BP-PF+AIS and BP-PF+AIS+IMM methods. This is confirmed by Table I, which reports the individual costs constituting the mean GOSPA error (averaged over time), i.e., the localization cost for correctly confirmed targets and the costs for missed and false targets. The larger number of false tracks created by the BP-PF+AIS and BP-PF+AIS+IMM methods is mainly due to the use of the heuristic described in [15] to model the generation of new targets, which was later superseded by the fully Bayesian BP-based tracking method proposed in [13].

Finally, Table II presents a comparison between the average computation times per time scan for all the methods. This comparison shows that the BP-PF+AIS method is the fastest method, even faster than the original VIMMJIPDA method that does not process the target-provided measurements. However, definite conclusions cannot be drawn from this analysis, given the different implementations, the different number of kinematic models used, and the different programming languages employed.

B. Scenario Considered in [9]

Next, we present results for a simulated scenario that is similar to the one considered in [9, Sec. VI-A]. Our scenario consists of nine targets that are moving with a constant velocity of 4 m/s. The starting points of the target trajectories are equally spaced on a circle with center $[0, 0]^{\mathrm{T}}$ and radius 4 km. The target trajectories and the radar sensor are depicted in Fig. 4. Unlike the scenario considered in the previous subsection, here the trajectories are deterministic — thus, they are equal for all simulation runs — and approximately cross each other in $[0, 0]^{\mathrm{T}}$. Five targets appear at $t = 0$ s and do not disappear, and the other four targets appear at $t = 40$ s and disappear at about $t = 32$ min. Six randomly selected targets provide AIS measurements between $t = 1.5$ min and $t = 31.5$ min. The number of AIS measurements provided by

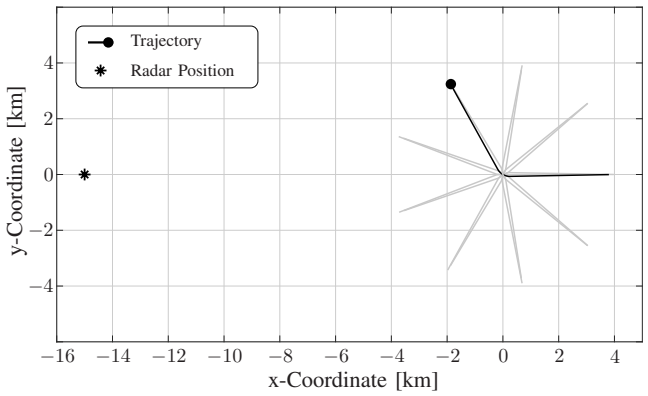

Fig. 4. Simulated scenario considered in [9, Sec. VI-A]. The star marks the position of the radar sensor, and the dot indicates the final position of the highlighted trajectory. The other trajectories are rotated (by multiples of 40 degrees) versions of the highlighted one.

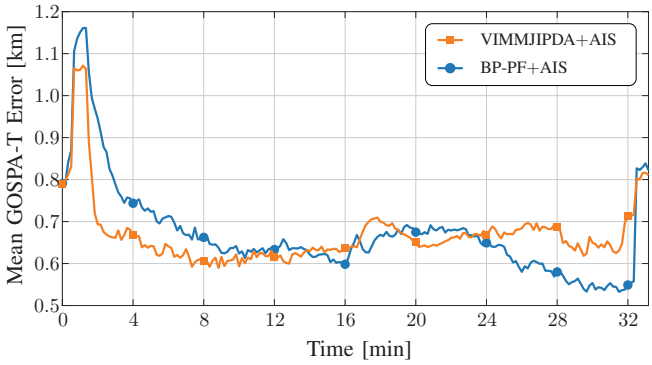

Fig. 5. Mean GOSPA-T error versus time for the simulated scenario considered in [9, Sec. VI-A].

a target during each time scan is Poisson distributed with mean 0.5 for three of the six targets and mean 1 for the other three targets. The time scan duration is set to 10 s. The AIS measurement noise is modeled as before. The radar detects a target with probability $P_{\mathrm{D}} = 0.5$, and it generates range-bearing measurements with a 2D zero-mean Gaussian measurement noise with covariance $\mathrm{diag}(250^2\ \mathrm{m}^2, 2.56^2\ \mathrm{deg}^2)$. The number of false alarms is Poisson distributed with mean 2. For this scenario, both the BP-PF+AIS and VIMMJIPDA+AIS methods use a single NCV model with driving noise variance set to $0.15^2\ \mathrm{m}^2\ \mathrm{s}^{-3}$. The parameters for the BP-PF+AIS method are set as in [9]. For the VIMMJIPDA+AIS method, we use the parameters reported in [1, Tab. III] with the exception of the clutter density set to $1.7{\times}10^{-9}\ \mathrm{m}^{-2}$, the unknown target rate set to $10^{-10}\ \mathrm{m}^{-2}$, and the parameters related to the radar measurement noise, that is, the range measurement variance set to $250^2\ \mathrm{m}^2$ and the bearing measurement variance set to $2.56^2\ \mathrm{deg}^2$.

As previously done in [9], we compare the VIMMJIPDA+AIS and BP-PF+AIS methods in terms of the mean GOSPA error for trajectories (GOSPA-T) [18] of order 2 and with cut-off parameter 500 m, averaged over 100 simulation runs. Compared to the GOSPA error, the GOSPA-T error additionally accounts for track switches by adding a switching penalty of 125 m. One can see in Fig. 5 that the VIM-

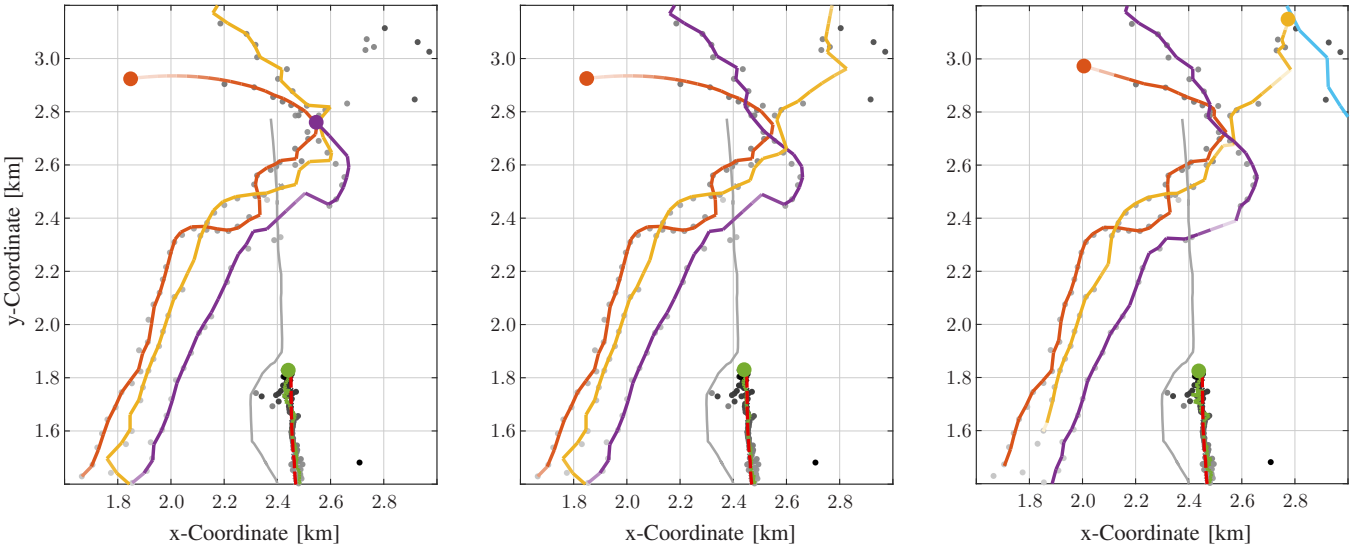

(a) VIMMJIPDA method (b) VIMMJIPDA+AIS method (c) BP-PF+AIS method

Fig. 6. Trajectories estimated by (a) the VIMMJIPDA method, (b) the VIMMJIPDA+AIS method, and (c) the BP-PF+AIS method using a real dataset acquired as part of the Autosea project [7]. The estimated trajectories are depicted in orange, yellow, purple, and green, with their final positions indicated by large dots. The transparency of the tracks is related to their existence probability: lighter (darker) colors correspond to lower (higher) existence probabilities. The red dashed line indicates the ground-truth trajectory of the slow-moving vessel. The gray line represents the known trajectory of the radar sensor. The gray/black dots and crosses indicate the radar and AIS measurements, respectively; the measurements become darker as time passes by. The blue line in the top-right corner of the rightmost panel is a false track created by the BP-PF+AIS method.

TABLE III
TIME-AVERAGED INDIVIDUAL COSTS CONSTITUTING THE MEAN GOSPA-T ERROR (IN METER) FOR THE SIMULATED SCENARIO CONSIDERED IN [9]. BOLD FONT HIGHLIGHTS THE LOWEST VALUE IN EACH COLUMN.

	LOCAL.	FALSE	MISSED	SWITCH
VIMMJIPDA+AIS	**249.9**	**138.3**	532.3	**9.5**
BP-PF+AIS	325.0	271.7	**394.8**	10.5

MJIPDA+AIS method outperforms the BP-PF+AIS method during approximately the first half of the simulation, that is, where the targets are well-separated. As the targets get closer, the difference between the GOSPA-T errors of the two methods becomes less significant. From minute 24, after the targets have crossed their paths, the BP-PF+AIS method outperforms the VIMMJIPDA+AIS method. This is due to the inability of the VIMMJIPDA+AIS method to continue tracking some of the targets after they crossed their paths, as demonstrated by the higher time-averaged missed cost component of the mean GOSPA-T error shown in Table III. On the other hand, the time-averaged localization and false costs of the VIMMJIPDA+AIS method are lower than those of the BP-PF+AIS method. In terms of average computation time, the BP-PF+AIS method is faster than the VIMMJIPDA+AIS method: it requires 0.61 s to process each time scan, whereas the VIMMJIPDA+AIS method requires 0.81 s.

IV. RESULTS FOR REAL DATA

Finally, we assess and compare the performance of the VIMMJIPDA, VIMMJIPDA+AIS, and BP-PF+AIS methods for a real dataset that was acquired as part of the Autosea project [7]. The scenario now consists of a radar sensor mounted onboard a semiautonomous surface craft and four unknown targets: a 30 m long slow-moving vessel consistently providing AIS measurements and three fast-moving rigid hull inflatable boats (RHIBs), one of which provides a single AIS measurement. The VIMMJIPDA and VIMMJIPDA+AIS methods employ three kinematic models as in [1] — two NCV models and one CT model — and use the parameters reported in [1, Tab. III]. The BP-PF+AIS method uses a single NCV model with driving noise variance set to 1.7^2 m^2 s^{-3}, which is higher than the driving noise variances used for the VIMMJIPDA and VIMMJIPDA+AIS methods, and also noticeably higher than the driving noise variance used for the BP-PF+AIS method in [1]. Results obtained with the BP-PF+AIS+IMM method using two NCV models are not reported because they are equivalent to those obtained with the BP-PF+AIS method.

Fig. 6 shows the trajectories estimated by the three methods as colored solid lines. The semiautonomous surface craft is sailing from north to south, and its trajectory, depicted as a gray solid line, is known. The unknown targets are traveling from south to north. The ground-truth trajectory of the slow-moving vessel, obtained by connecting its AIS measurements, is also depicted as a red dashed line; the ground-truth trajectories of the three fast moving RHIBs are not available. Differently from the results reported in [1], Fig. 6 shows that the BP-PF+AIS method performs better than the VIMMJIPDA method, which loses track of one of the three RHIBs when their paths cross, and performs almost identically to the VIMMJIPDA+AIS method. Despite using only a single NCV model, the BP-PF+AIS method is able to estimate the trajectories of all the targets with high accuracy. The drawbacks of

using a higher driving noise variance than the driving noise variances used for the VIMMJIPDA and VIMMJIPDA+AIS methods and for the BP-PF+AIS method in [1], are manifested by the facts that the estimated trajectory for the slow-moving vessel exhibits abrupt changes of direction, and that a false track is created in the top-right corner of the considered area.

V. Conclusion

Recently, an extension of the VIMMJIPDA method that is able to include target-provided measurements was proposed in [1]. The effectiveness of this approach was validated in [1] through a comparison with the BP-PF+AIS method presented in [8], [9], whose code is not publicly available. In this paper, we presented the results of an experimental comparison using the implementation of the BP-PF+AIS method originally used in [8], [9] as well as the BP-PF+AIS+IMM method from [11]. Simulation results showed that the VIMMJIPDA+AIS method outperforms the BP-PF+AIS and BP-PF+AIS+IMM methods when the targets are well-separated, whereas the BP-PF+AIS and BP-PF+AIS+IMM methods have performance advantages in the case of closely spaced targets. The reason why the VIMMJIPDA+AIS method performs worse in the latter case is likely the limited performance of the data association scheme based on Murty's algorithm, which struggles when targets are closely spaced. Improvements to the VIMMJIPDA+AIS method can be obtained by resorting to the variational approximation method presented in [19]. However, due to its use of a CT kinematic model, the VIMMJIPDA+AIS method generally provides more accurate estimates when the targets perform sharp maneuvers. On the other hand, the BP-based data association algorithm used within the BP-PF+AIS and BP-PF+AIS+IMM methods tends to produce better results in challenging tracking environments with tighter target spacings [14]. Finally, results obtained with a real dataset showed that the BP-PF+AIS method using a single NCV kinematic model whose driving noise parameter is sufficiently high can track the agile RHIBs with performance comparable to that obtained with the VIMMJIPDA+AIS method.

References

[1] A. G. Hem and E. F. Brekke, "Variations of joint integrated data association with radar and target-provided measurements," *J. Adv. Inf. Fusion*, vol. 17, no. 2, pp. 97–115, Dec. 2022.

[2] E. F. Brekke, A. G. Hem, and L.-C. N. Tokle, "Multitarget tracking with multiple models and visibility: Derivation and verification on maritime radar data," *IEEE J. Ocean. Eng.*, vol. 46, no. 4, pp. 1272–1287, Oct. 2021.

[3] H. A. P. Blom and Y. Bar-Shalom, "The interacting multiple model algorithm for systems with Markovian switching coefficients," *IEEE Trans. Autom. Control*, vol. 33, no. 8, pp. 780–783, Aug. 1988.

[4] E. Tu, G. Zhang, L. Rachmawati, E. Rajabally, and G.-B. Huang, "Exploiting AIS data for intelligent maritime navigation: A comprehensive survey from data to methodology," *IEEE Trans. Intell. Transp. Syst.*, vol. 19, no. 5, pp. 1559–1582, May 2018.

[5] M. Strohmeier, M. Schafer, V. Lenders, and I. Martinovic, "Realities and challenges of NextGen air traffic management: The case of ADS-B," *IEEE Commun. Mag.*, vol. 52, no. 5, pp. 111–118, May 2014.

[6] H. Chen, T. Kirubarajan, and Y. Bar-Shalom, "Performance limits of track-to-track fusion versus centralized estimation: Theory and application," *IEEE Trans. Aerosp. Electron. Syst.*, vol. 39, no. 2, pp. 386–400, Apr. 2003.

[7] E. F. Brekke, E. F. Wilthil, B.-O. H. Eriksen, D. K. M. Kufoalor, Ø. K. Helgesen, I. B. Hagen, M. Breivik, and T. A. Johansen, "The Autosea project: Developing closed-loop target tracking and collision avoidance systems," *J. Phys. Conf. Ser.*, vol. 1357, p. 012020, Oct. 2019.

[8] D. Gaglione, P. Braca, and G. Soldi, "Belief propagation based AIS/radar data fusion for multi–target tracking," in *Proc. FUSION-18*, Cambridge, UK, Jul. 2018.

[9] D. Gaglione, P. Braca, G. Soldi, F. Meyer, F. Hlawatsch, and M. Z. Win, "Fusion of sensor measurements and target-provided information in multitarget tracking," *IEEE Trans. Signal Process.*, vol. 70, pp. 322–336, Dec. 2021.

[10] Online code repository: Variations of joint integrated data association with radar and target-provided measurements. [Online]. Available: https://doi.org/10.24433/CO.4125751.v2

[11] G. Soldi, F. Meyer, P. Braca, and F. Hlawatsch, "Self-tuning algorithms for multisensor-multitarget tracking using belief propagation," *IEEE Trans. Signal Process.*, vol. 67, no. 15, pp. 3922–3937, Aug. 2019.

[12] K. G. Murty, "An algorithm for ranking all the assignments in order of increasing cost," *Oper. Res.*, vol. 16, no. 3, pp. 682–687, Jun. 1968.

[13] F. Meyer, T. Kropfreiter, J. L. Williams, R. Lau, F. Hlawatsch, P. Braca, and M. Z. Win, "Message passing algorithms for scalable multitarget tracking," *Proc. IEEE*, vol. 106, no. 2, pp. 221–259, Feb. 2018.

[14] J. Williams and R. Lau, "Approximate evaluation of marginal association probabilities with belief propagation," *IEEE Trans. Aerosp. Electron. Syst.*, vol. 50, no. 4, pp. 2942–2959, Oct. 2014.

[15] F. Meyer, P. Braca, F. Hlawatsch, and P. Willett, "A scalable algorithm for tracking an unknown number of targets using multiple sensors," *IEEE Trans. Signal Process.*, vol. 65, no. 13, pp. 3478–3493, Jul. 2017.

[16] Y. Bar-Shalom, X. R. Li, and T. Kirubarajan, *Estimation with Applications to Tracking and Navigation*. New York, NY, USA: Wiley, 2001.

[17] A. S. Rahmathullah, Á. F. García-Fernández, and L. Svensson, "Generalized optimal sub-pattern assignment metric," in *Proc. FUSION-17*, Xi'an, China, Jul. 2017.

[18] Á. F. García-Fernández, A. S. Rahmathullah, and L. Svensson, "A metric on the space of finite sets of trajectories for evaluation of multi-target tracking algorithms," *IEEE Trans. Signal Process.*, vol. 68, pp. 3917–3928, Jun. 2020.

[19] J. Williams, "An efficient, variational approximation of the best fitting multi-Bernoulli filter," *IEEE Trans. Signal Process.*, vol. 63, no. 1, pp. 258–273, Jan. 2015.